Pergamon

Tetrahedron 55 (1999) 1505–1516

TETRAHEDRON

How Kinetically Accessible is an RNA Target for Hybridization with an Antisense Oligo? A Lesson from an RNA Target which is as Small as a 20mer

Nitin Puri and Jyoti Chattopadhyaya*

Department of Bioorganic Chemistry, Box 581, Biomedical Center, University of Uppsala, S-751 23 Uppsala, Sweden

E-mail: jyoti@bioorgchem.uu.se. Fax: +4618-554495

Received 9 October 1998; accepted 3 December 1998

Abstract: A 20mer RNA (**1**), characterized as a duplex with two A•A mismatch basepairs and four tandem G•U wobble basepairs, was targeted at the first A•A internal loop by nonameric 5'-Polyarene DNA-conjugates. For comparison, its DNA counterpart (**10**), which was found to form a hairpin with one A•A mismatch and a four nucleotide loop, was targeted at the single stranded loop starting from the A•A internal loop. The secondary structure of the duplex RNA (**1**) could not be disrupted by the DNA-conjugates while the hairpin DNA (**10**) was found to hybridize successfully, thereby showing the intrinsic ability of RNA (compared to DNA counterpart) to fold into a tertiary structure that is kinetically difficult to access for heteroduplex formation by an antisense ODN.

Keywords: antisense target; polyarenes; DNA conjugates.

Introduction

One of the primary pitfalls of the antisense strategy lies in the selection of the kinetically accessible target sequences because of the secondary and tertiary structures of mRNA. Using a 47-nucleotide RNA transcript of the Ha-*ras* gene as the target, it has been shown[1] that the folded nature of the RNA structure profoundly inhibits duplex formation with an antisense oligodeoxynucleotides (ODN). Different methodologies[2-8] have been used in identifying potent antisense target sequences for heteroduplex formation. Southern and co-workers have used a DNA array with 1938 different ODNs to measure the potential for heteroduplex formation with the first 122 nucleotides (nt) of rabbit β-globin mRNA.[2] Essentially, *only one* of these ODNs annealed efficiently to the target and showed good inhibition in a translation experiment, showing that the kinetic availability of the target RNA sequence is very few. Different randomized libraries of antisense ODNs in combination with RNase H have been used for identifying regions on mRNA accessible to hybridization with these ODNs[3-5]: Eckstein and co-workers[3] used a randomized (4^{10}) ODN (10mer) library to find *only six* accessible sites in the in vitro RNA transcript (fragment 550-2149) of human acetylcholinesterase. Lima *et al.*[4] directed backbone optimized ODNs generated from randomized (4^{10}) ODN (10mer) library against two folded RNA fragments (200 and 370 nt long) spanning the 5'-region of a hepatitis C viral RNA

0040-4020/99/$ - see front matter
PII: S0040-4020(98)01129-6

(440 nt). Using this approach, they were able to identify *only two* preferred sites of high affinity heteroduplex hybridization which caused *in vitro* translational arrest. Essentially the same approach was used by Ho *et al.*[5] in identifying *eight accessible regions* in the 1253 nt angiotensin type-1 receptor (AT_1) mRNA using a semirandom ($4x4^9$) chimeric library of methoxyribonucleotides and ODNs (10mer). Phosphorothioate ODNs (10mer) directed against all eight identified regions by this approach inhibits the expression of AT_1 receptor not only in cell culture but also in an animal model.

Toulmé and co-workers[6] have targeted nucleic acids by antisense ODNs using an *in vitro* selection approach. Using this approach they have identified *19 aptastrucs* (*i.e.*, aptamers against an RNA structure) from a library of oligomers (66mer with a window of 30 random positions in the middle, *i.e.*, about 10^{14} different molecules) that bind to 59 nt long TAR RNA element of HIV-1 with a dissociation constant in the nanomolar range.[7] Another approach[8] used by Strauss and Lieber was the generation of a library of human growth hormone (hGH) mRNA specific ribozymes with random sequences of 13 nt on both sides of the hammerhead using a expression cassette for the ribozyme gene (10^9 plasmid clones). They found that *in vitro* out of 156 potential cleavage sites of the hGH target RNA (1,600 nt) *only seven* were cleaved by the library of ribozymes.

We have been interested in evaluating how different RNA structures, *i.e.*, a duplex vis-à-vis hairpin, differ in their behaviour towards being hybridized by an antisense ODN such as the 5'-polyarene DNA-conjugates.[9,10] In this report, these DNA-conjugates were targeted to a palindromic 20mer RNA (**1**) (Figs. 1 & 2) which forms a duplex with tandem G•U wobble[11-13] and A•A mismatch[14] basepairs, and it was found that the RNA target (**1**) was kinetically inaccessible for hybridization. On the other hand, the DNA counterpart (**10**) (Figs. 1 & 2) which forms a hairpin with a four base loop and a A•A mismatch[15,16] was successfully capable of being hybridized at its loop by the DNA-conjugates. The secondary structures of both RNA (**1**) and DNA (**10**) are conclusively identified using concentration dependent thermal studies, PAGE and CD.

1: 5'-r(UUAACAUGUUUGGACAAGUU)3'
2: 5'-r(UUAACAUGUUUGGACAAG)3'
3: 5'-r(AACAUGUUUGGACAAGUU)3'
4: 3'-r(UACAAACCU)-5'
5: 5'-r(CAUGUUUGGA)-3'

10: 5'-d(TTAACATGTTTGGACAAGTT)3'
11: 5'-d(TTAACATGTTTGGACAAG)3'
12: 5'-d(AACATGTTTGGACAAGTT)3'
13: 3'-d(TACAAACCT)-5'
14: 5'-d(CATGTTTGGA)-3'

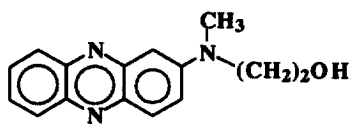

6

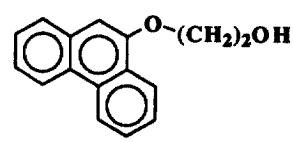

7

DNA-conjugate 8-9: 3'-d(TACAAACCT)-5'-OP(O_2)-X)
(X = corresponding alkoxy moiety of the alcohols 6-7)

Fig. 1 DNA and RNA single strands shown with the DNA-conjugates used.

RESULTS

Thirteen different DNA constructs reported[10] from our laboratory have been targeted against ssRNA to test their use in the antisense strategy. The ability of these DNA constructs to form DNA-DNA duplex has also been evaluated in order to compare with those of DNA-RNA heteroduplex.[9,10] A small 20mer RNA was chosen to test the efficiency of these DNA constructs in disrupting the secondary structure of the target. We envisioned that the choice of a relatively small ssRNA would enable us to identify its structural features (through temperature dependent UV/VIS, CD and PAGE), which make it an accessible or inaccessible target. The second consideration for choosing a smaller RNA target was that it provides an easy means to prepare its mutants by standard solid-phase chemistry. Our choice of ssRNA was also based on its ability to intermolecularly assemble to form a homoduplex or to intramolecularly fold to form a hairpin. Hence, we chose a palindromic RNA sequence (**1**) (Fig. 1), 5'-r(UUAACAUGUUUGGACAAGUU)3', whose secondary structure was theoretically analyzed using the mfold algorithm[17,18], which is parametrized on the basis of "nearest-neighbour" thermodynamics.

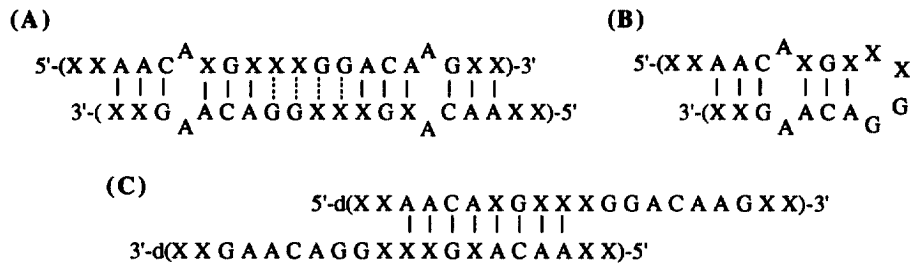

Fig. 2 Possible stable secondary structures of 20mer target RNA **1** (X = U) & DNA **10** (X = T).

(A) Characterization of RNA (1) as a duplex.

Three possible secondary structures can be envisioned for 20mer RNA (**1**) (Figs. 1 & 2): Duplex (**A**) with two A•A mismatch basepairs and four successive G•U wobble basepairs along with twelve fully matched basepairs and two 5'-dangling uridines. The solution structure of A•A mismatch has been reported by NMR.[14] G•U basepairing has been shown by NMR[11] and by X-ray crystallography[12,13] to adopt a wobble form of basepairing with little effect on the global structure of the A-RNA. The second possible structure for RNA (**1**) is a hairpin (**B**) (Fig. 2) with one A•A mismatch along with six fully matched basepairs in the stem part and a four nucleotide hairpin loop. The 5'-end of hairpin (**B**) has two dangling uridines. Duplex (**C**) could also be possible with eight fully matched basepairs in a row without any mismatch interruptions with two and ten nucleotide residues dangling at the 5'- and 3'-ends respectively in each strand. The secondary structure adopted by RNA (**1**) was resolved by a series of studies involving concentration-dependency of T_m, estimation of thermodynamic stability, PAGE and CD.

Table 1. Concentration dependent thermal melting (T_m in° C) of 20mers RNA (**1**) and DNA (**10**).

	1μM	5μM	10μM
20mer RNA (**1**)	38.9	42.0	43.6
20mer DNA (**10**)	45.5	45.8	46.2

(a) Concentration dependent study of thermal stability of RNA (1).

RNA (**1**) existing as the duplex (**C**) (Fig. 2) was ruled out by comparison of its thermal stability (T_m = 38.9° C) with those of two analogous 18mer RNAs (**2**) (T_m = 28.9° C) and (**3**) (T_m = 35.9° C) (Fig. 1) in which two uridine bases were removed from 3'- and 5'-ends respectively. The 18mer RNA (**2**) (Fig. 1) showed more destabilization than the isomeric RNA (**3**) (Fig. 1) as compared to the parent 20mer RNA (**1**), implying that the two uridine bases at the 3'-end of RNA (**1**) are contributing significantly (by being involved in basepairing) towards its stability. This suggests that (**A**) or (**B**) in Fig. 2 are the likely secondary structures for RNA (**1**).

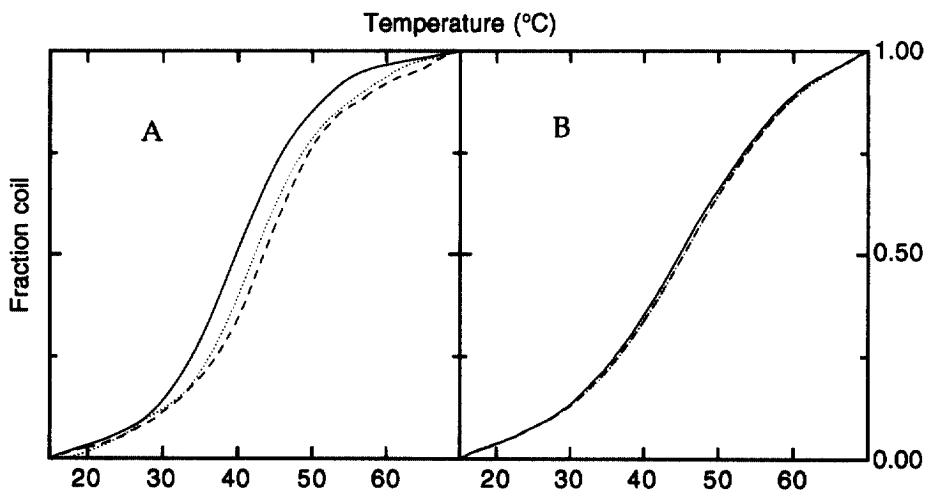

Figure 3. Fraction coil versus temperature profile of 20mer RNA hairpin (**1**) (Panel **A**) and 20mer DNA duplex (**10**) (Panel **B**) at varying oligo concentrations: 1 μMol (———), 5 μMol (.....) and 10 μMol (- - - -) in 1.3 ml of buffer A.

A concentration dependent T_m study of 20mer RNA (**1**) was performed in 20 mM PO_4^{3-}, 1.0 M NaCl buffer at pH 7.3 (buffer A) with the temperature range 15° - 70° C. All melting curves showed a clear monophasic dissociation (Fig. 3). The 20mer RNA (**1**) showed significant change in thermal stability (Table 1 & Fig. 3, Panel A) with change in concentration. This rules out the adoption of hairpin (**B**) structure by RNA (**1**), suggesting that it takes up most probably the duplex structure (**A**) (since the hairpin structure follows first-order kinetics,[19,20] whereas duplex melting follows the second order[19]).

(b) Calculated thermodynamic stabilities of RNA (1).

The free energies of folding at 25° C of the three contributing structures of the 20mer RNA (1) (Fig. 2) calculated using RNA mfold algorithm (ver 3.0) (based on the nearest-neighbour thermodynamic parameters determined by Turner and co-workers[21]) were as follows: duplex (A): -18.4 kcal/mol, hairpin (B): -3.0 kcal/mol and duplex (C): -12.7 kcal/mol. Here RNA (1) is predicted to exist as duplex (A) which is its experimental structure as determined by this work.

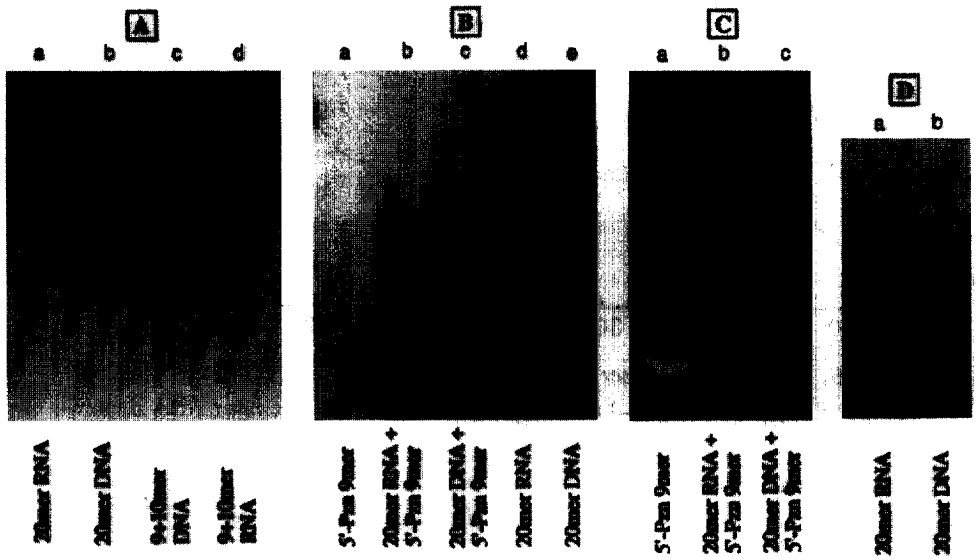

Figure 4. (A) 15% native PAGE pattern showing electrophoretic mobility of RNA duplex (1) (lane a), DNA hairpin (10) (lane b), DNA duplex (13)•(14) (lane c) and RNA duplex (4)•(5) (lane d). (B) 15% native PAGE pattern viewed under UV light of 254 nm showing electrophoretic mobility of 5'Pzn-9mer (8) (lane a), mixture of RNA duplex (1) & 5'Pzn-9mer (8) (lane b), a complex of DNA hairpin (10) & 5'Pzn-9mer (8) (lane c), RNA duplex (1) (lane d) and DNA hairpin (10) (lane e). (C) 15% native PAGE pattern viewed under UV light of 366 nm showing electrophoretic mobility of 5'Pzn-9mer (8) (lane a), mixture of RNA duplex (1) & 5'Pzn-9mer (8) (lane b) and a complex of DNA hairpin (10) & 5'Pzn-9mer (8) (lane c). (D) 20% denaturing PAGE of RNA duplex (1) (lane a) and DNA hairpin (10) (lane b).

(c) PAGE of RNA (1).

The secondary structure of RNA (1) (Fig. 4, Panel A, lane a) were further confirmed by running experiments on 15% polyacrylamide gels under native conditions[22] at 5° C. 9+10mer RNA duplex (4)•(5) (Fig. 4, Panel A, lane d) was also run for comparison. RNA duplex (4)•(5) [*i.e.*, 17 phosphates] showed faster electrophoretic mobility than RNA (1) in its native form [*i.e.*, 38 phosphates in the duplex form (A) and 19 phosphates in the hairpin form (B)], thereby implying that the secondary structure of RNA (1) has more charges than 9+10mer RNA duplex (4)•(5), which rules out its adoption of the hairpin structure (B). This is consistent with what is known[22,23] about

electrophoretic mobilities of isomeric DNA existing in the hairpin or the duplex forms or as their equilibrium mixture.

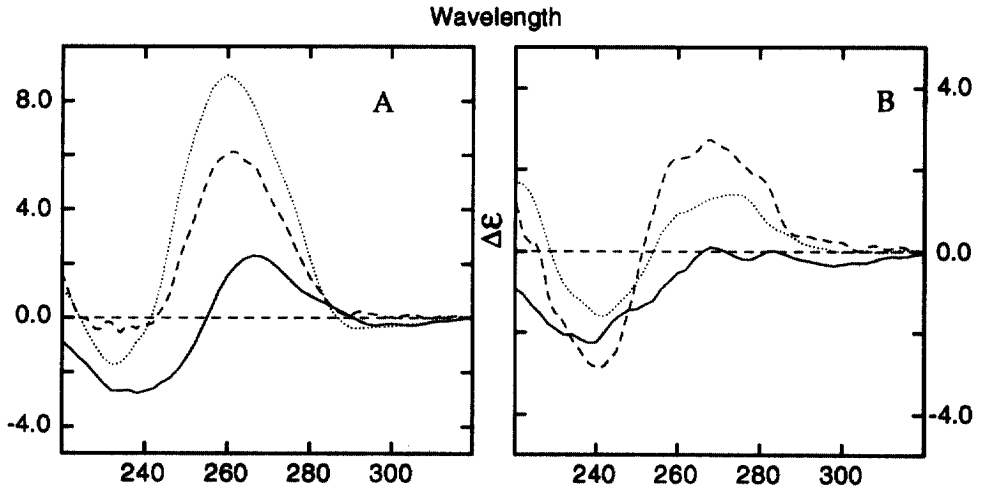

Figure 5. CD spectra of 20mer RNA duplex (1) (Panel A) and 20mer DNA hairpin (10) (Panel B) at 7° C (.....) and 55° C (———). CD spectra of RNA duplex (4)•(5) (- - - -) (Panel A) and DNA duplex (13)•(14) (- - - -) (Panel B) are also shown for comparison.

(d) CD spectra of RNA (1).

To characterize the structure of 20mer RNA (1), its CD spectra (Fig. 5, Panel A) was recorded at 10 μmol concentration using same buffer conditions as for the thermal study. Fig. 5 also shows, for comparison, the CD spectra of an RNA duplex (4)•(5) (Panel A) representing A-RNA form. The CD spectra (Fig. 5, Panel A) of RNA (1) showed that its conformation was more characteristic of A-RNA conformation showing a large positive molar ellipticity above 260 nm. This was also concluded by comparing with the CD spectra of the A-form RNA duplex (4)•(5).

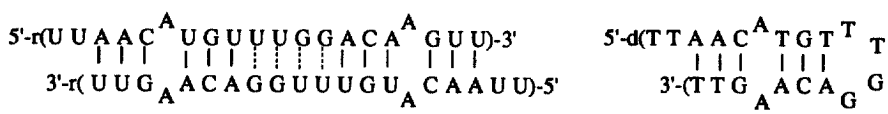

Fig. 6 Determined stable secondary structures of 20-mer target RNA **1** & DNA **10**.

(B) Targeting RNA secondary structures by Antisense ODNs.

From the concentration dependent study of thermal stability and PAGE of RNA (1) we can conclude that it adopts a secondary structure as in duplex (A) (Figs. 2 & 6). The effectiveness of disruption of the secondary structure of RNA duplex (1) by our reported DNA constructs[10] was

tested. Out of the thirteen different DNA constructs, the DNA-conjugates having *N*-(2-hydroxyethyl)phenazine (Pzn) (**6**) and 9-(2-hydroxyethoxy) phenantharene (Phn) (**7**) (Fig. 1), tethered through the 5'-phosphate of 9mer DNA-conjugates (**8**) and (**9**) respectively, were used for further investigations as they had shown[9,10] the best stabilizations with both 10mer RNA (**5**) and DNA (**14**) complementary targets (Fig. 1).

In a recent review,[24] Toulmé and co-workers have highlighted taking advantage of unpaired bases (as in bulges, loops) to minimize the thermodynamic penalty of disruption of the target structure. Also complementary DNA has been found to be able to invade duplexes in ribosomal RNA using internal loops within the helices.[25] To use this information our DNA-conjugates were targeted to the 20mer RNA (**1**) starting at the A•A mismatch site and along the stem containing the tandem G•U wobble basepairs. A solution in buffer A of 1:1 mixture of the DNA-conjugates and RNA (**1**) was heated to 70° C, then slowly cooled to 4° C and incubated overnight. Their melting curves showed a clear monophasic dissociation exactly like the one showed by the melting of just the RNA duplex (**1**). Hence, it was difficult to confirm the formation of the heteroduplex.

To investigate the formation of the heteroduplex, a 1:1 mixture of 5'Pzn-9mer (**8**) and RNA (**1**) was incubated (as reported above) in buffer A (25 μl) and PAGE was run under native conditions (Figs. 4, Panels B and C, lane b). For comparison both 5'Pzn-9mer (**8**) (Fig. 4, Panel B and C, lane a) and RNA (**1**) (Fig. 4, Panel B, lane d) were also run in separate lanes after incubation. Under UV light of 254 nm, it was seen that the electrophoretic mobility of the visible mixture of 5'Pzn-9mer (**8**) and RNA (**1**) (Fig. 4, Panel B, lane b) was the same as that for RNA (**1**) alone (Fig. 4, Panel B, lane d). Also under UV light of 366 nm, it was clearly seen that the 5'Pzn-9mer (**8**) had not complexed with RNA (**1**) (Fig. 4, Panel C, lane b) and had a electrophoretic mobility close to that of pure 5'Pzn-9mer (**8**) (Fig. 4, Panel C, lane a). It was also observed that the electrophoretic mobility of 5'Pzn-9mer (**8**) was smeared out (Fig. 4, Panel C, lane b) when run as a mixture of 5'Pzn-9mer (**8**) and RNA (**1**) possibly because of a dynamic equilibrium of weak associations and dissociations between them. Clearly the DNA-conjugates (**8**) and (**9**) did not form a heteroduplex structure with 20mer RNA (**1**) owing to the high thermodynamic stability of its folded structure.

(C) Differences in the folding states of a DNA and an RNA with the same primary sequence.

The kinetic inaccessibility of RNA (**1**) to DNA-conjugates prompted us to evaluate the ability of its DNA counterpart (**10**) (Fig. 1) to form a homoduplex with 5'-polyarene DNA. We argued that this might highlight the role of 2'-hydroxyl group in the ribose sugar in RNA (**1**) in disallowing disruption of its tertiary structure by antisense ODNs.[26] The secondary structure of DNA (**10**) was analyzed using the mfold algorithm. Like in the case of RNA (**1**) three possible secondary structures can be envisioned for DNA (**10**) (Fig. 2): Duplex (**A**) with two A•A mismatch basepairs and four successive G•T wobble basepairs along with twelve fully matched basepairs and two 5'-dangling thymidines. The solution structure of A•A mismatch has been reported by NMR.[15,16] G•T basepairing has been shown[27] by crystal structure analysis to adopt a wobble structure in B-DNA showing only localized changes in the helix compared to the isomorphous parent G•C compound.

Duplex (**A**) can be formed by DNA (**10**) as it has a palindromic sequence. The second possible structure for DNA (**10**) is a hairpin (**B**) (Fig. 2) with one A•A mismatch along with six fully matched basepairs in the stem part and a four nucleotide hairpin loop. The 5'-end of hairpin (**B**) has two dangling thymidines. Duplex (**C**) (Fig. 2) could also be possible with eight fully matched basepairs in a row without any mismatch interruptions with two and ten nucleotide residues dangling at the 5'- and 3'-ends respectively in each strand. The correct secondary structure was resolved by a series of studies involving concentration-dependency of T_m, estimation of thermodynamic stability, PAGE and CD of DNA (**10**).

(a) Concentration dependent study of thermal stabilities of DNA (10).

The adoption of the structure (**C**) by DNA (**10**) was eliminated by comparison of its thermal stability (T_m = 37.7° C) with those of two 18mer DNAs (**11**) (T_m = 31.2° C) and (**12**) (T_m = 36.5° C) (Fig. 1), in which two thymidine bases were removed from 3'- and 5'-ends respectively of DNA (**10**). Since the 18mer DNA (**12**) showed thermal stability closer to parent DNA (**10**), the two thymidine bases at the 3'-end are contributing towards its stability, suggesting that (**A**) or (**B**) in Fig. 2 are the likely secondary structures for DNA (**10**). A concentration dependent T_m study of 20mer DNA (**10**) was carried out in buffer A with the temperature range 15° - 70° C. All melting curves showed a clear monophasic dissociation. The 20mer DNA (**10**) showed no significant change in the thermal stability (Fig. 3, panel B & Table 1) as the concentration was changed, implying that it is following first-order kinetics in forming its secondary structure. It can be derived from the above that DNA (**10**) forms a hairpin as depicted in the structure (**B**) (Figs. 2 & 6).

(b) Calculated thermodynamic stabilities of DNA (10).

For 20mer DNA (**10**), the calculated free energy of folding for the contributing structures (Fig. 2) at 25° C were determined by DNA mfold program (ver 3.0) (using parameters determined by SantaLucia[28]), duplex (**A**): -9.0 kcal/mol, hairpin (**B**): -3.2 kcal/mol and duplex (**C**): -11.7 kcal/mol. Here the lowest energy structure predicted for DNA (**10**) was duplex (**C**). As DNA (**10**) exists in the hairpin form (**B**), hence the possible reason for the discrepancy could be owing to the reason that the mfold algorithm does not take into account of the 3'-dangling single stranded ends on both the strands of duplex (**C**).

(c) PAGE of DNA (10).

Further confirmation of DNA (**10**) (Fig. 4, Panel A, lane b) adopting the hairpin structure (B) was performed by PAGE experiments under native conditions[22] at 5° C. DNA duplex (**13**)•(**14**) (Fig. 4, Panel A, lane c) was also run for comparison. The electrophoretic mobility (Fig. 4, Panel A, lane b) of DNA (**10**) was faster than that of RNA (**1**) (Fig. 4, Panel A, lane a), thereby showing the combined effect of the phosphate charges as well as the 2'-OH group effect in the folding of the latter. These two effects could be separately understood by running PAGE under denaturing conditions (Fig 4, Panel D). The effect of the 2'-OH group was clearly visible as a retarding element in the PAGE of RNA (1) (Fig 4, Panel D, lane a) which displayed a slower electrophoretic mobility

than DNA (**10**) (Fig 4, Panel D, lane b) under denaturing conditions. Under native conditions, the DNA duplex (**13**)•(**14**) (Fig 4, Panel A, lane c) showed the same electrophoretic mobility as DNA (**10**) (Fig 4, Panel A, lane b). This implies that DNA (**10**) [*i.e.*, 38 phosphates in the duplex form (**A**) and 19 phosphates in the hairpin form (**B**)] has approximately the same number of charges as DNA duplex (**13**)•(**14**) [*i.e.*, 17 phosphates]. This data corroborates the adoption of hairpin structure (**B**) by DNA (**10**) (Figs. 2 & 6).

(d) CD spectra of DNA (10).

To characterize the structure of 20mer DNA (**10**), its CD spectra (Fig. 5, Panel B) was recorded at 10 μmol concentration. Fig. 5 also shows, for comparison, the CD spectra of DNA duplex (**13**)•(**14**) (Panel B) representing B-DNA form. The CD spectra (Fig. 5, Panel B) of DNA (**10**) was very similar to the DNA duplex, in having positive and negative molar ellipticity of moderate magnitude at wavelengths above 220 nm and a crossover point between 248 nm and 262 nm, characteristic of the B-DNA conformation.[29] It is difficult, in general, to distinguish between the hairpin and the duplex structure of a DNA using only CD as a technique, since both of them have double-stranded regions in the B-DNA form.[30] This has been proven by a combined NMR and CD studies on an equilibrium mixture of duplex-hairpin forms of a mismatched duplex [5'd(CGCGATTCGCG)3'], where the NMR showed various populations of hairpin versus duplex forms at different salt concentrations, while their CD was remarkably similar, thereby implying that the loop part of the hairpin contributes very insignificantly to the CD spectrum of B-type of DNA duplex.[30]

(D) Targeting of DNA hairpin (10) by antisense ODNs.

Our DNA-conjugates were targeted in the DNA hairpin (**10**) starting from the A•A internal loop in the ascending stem site and covering the complete single stranded loop. A 1:1 mixture of the DNA-conjugates and DNA (**10**) was incubated (as reported for RNA (**1**)) in buffer A overnight. Their melting curves showed a clear monophasic dissociation exactly like the one showed by the melting of just the hairpin (**10**). Hence using UV spectroscopy it was difficult to ascertain the formation of the heteroduplex.

Henceforth, the formation of the heteroduplex was investigated by PAGE. A 1:1 mixture of 5'Pzn-9mer (**8**) and DNA (**10**) (as reported above) was incubated in buffer A (25 μl) and PAGE was run under native condition. For comparison, both 5'Pzn-9mer (**8**) (Fig. 4, Panels B and C, lane a) and DNA (**10**) (Fig. 4, Panel B, lane e) were also run in separate lanes after incubation. Under UV light of 254 nm it was seen that the electrophoretic mobility of the visible complex of 5'Pzn-9mer (**8**) and DNA (**10**) (Fig. 4, Panel B, lane c) was considerably retarded than that for the DNA (**10**) alone (Fig. 4, Panel B, lane e). The hybridization of 5'Pzn-9mer (**8**) to DNA (**10**) was clearly seen under UV light of 366 nm where fluorescent band due to Pzn of (**8**) was visible at the same electrophoretic mobility (Fig. 4, Panel C, lane c) as the UV absorption band for the 5'Pzn-9mer (**8**) and DNA (**10**) complex (Fig. 4, Panel B, lane c). Clearly this shows the effective complexation of the DNA-

conjugate (**8**) with 5' stem site (with A•A internal loop) and the single stranded loop of the DNA hairpin (**10**).

Discussion

The observed complexation of DNA-conjugates with the DNA hairpin (**10**) supports the model where the loop structure promotes hybridization on the 5' side of the loop.[1] However the inability of the DNA-conjugates to bind to the RNA duplex (**1**), which is as small as a 20mer, was likely due to the kinetic inaccessibility of the folded RNA target in its single-stranded form or due to the inability of the DNA-conjugates to strand invade the RNA duplex (**1**). This is the smallest RNA so far reported that has its own thermodynamically preferred 3D structure that cannot be disrupted by competing intermolecular hybridization with a potential antisense ODN.

The reported free-energy increments for internal GG/UU[21] and GG/TT[31] wobble basepairs are -0.4 kcal/mol and 0.7 kcal/mol respectively. One explanation why the RNA (**1**) forms a duplex whereas DNA (**10**) forms a hairpin is because of the fact that tandem G•U wobble basepairing stablizes the free energy of the RNA structure as a duplex by 2.6 kcal/mol while tandem G•T wobble basepairing in DNA destabilizes it by 2.4 kcal/mol. Clearly the thermodynamic stability of the G•U wobble basepairs in RNA (**1**) does not allow the antisense ODN to bind to the target. The differences in the stability and form of the tertiary structures taken up by DNA and RNA could be the effect of the 2'-OH on the sugar in RNA and the C-5 methyl group on the thymine base in DNA. The C-5 methyl group in DNA has been shown[26] to stabilize duplex by 0.17-0.28 kcal/mol by increasing the base stacking proficiency. However, it is difficult to assess the contribution of the 2'-OH in RNA (**1**) and C-5 methyl group in dT of DNA (**10**) towards the formation of their respective tertiary structures.

Though less than the regular Watson-Crick basepairs, the prevalence of G•T/U basepairing in nucleic acid secondary structures is significant.[32] Hence they would be useful target sites for antisense ODNs. However from this work it can be derived that targeting nucleic acid tertiary structures with large stretches of tandem G•U basepairing by antisense ODNs is not kinetically viable.

Conclusion

Earlier studies from many laboratories have clearly highlighted on how very few sites (~ 2-10) are actually accessible on a large RNA (200-1600 nt) even when a large library (4^{10}) of antisense ODN are targeted onto it. The present analytical methods can not address the issue of how those large RNA targets are actually folded or why so few single stranded sites are kinetically accessible. In this work, we selected a small 20mer RNA system where it has been possible to show that it forms a duplex vis-à-vis its DNA counterpart, which forms a hairpin. It has been demonstrated that this 20mer RNA is not kinetically accessible to form a heteroduplex with the antisense 5'-polyarene DNA-conjugates, whereas its DNA counterpart can successfully form a homoduplex, thereby showing the intrinsic aptitude of RNA to fold into a complex thermodynamically stable tertiary structure that is

simply not kinetically available in the single stranded form for complexing with a potential antisense ODN.

Experimental

The synthesis of RNA (1) was performed by solid-phase amidite chemistry.[33] The reversed-phase HPLC purification of the 20mer RNA (1) did not give a clear separation; hence RNA (1) was purified using 20% polyacrylamide gel electrophoresis. The gel fragments with the purified RNA was extracted overnight using 0.25 M CH_3COONa buffer. The extracted RNA was filtered and desalted by centrifugation using Centricon™ concentrators and then passed through Dowex H^+. The synthesis and purification of DNA (10) has been reported earlier.[9] Melting measurements were carried out using a PC-computer interfaced Perkin Elmer UV/VIS spectrophotometer Lambda 40 with PTP-6 peltier temperature controller. The CD spectra were recorded using a JASCO J41-A Spectropolarimeter.

Gel Electrophoresis. Native and denaturing PAGE were carried out on gels (15 X 20 X 0.15 cm) at 5° C and rt. respectively. The 15% polyacrylamide native gel (obtained from a solution of 19% acrylamide, 1% bis(acrylamide), 10 mM Tris.HCl, 10 mM Boric acid, 0.1 mM EDTA and 0.07% ammonium persulfate, pH 7.5) in TBE buffer (10 mM Tris.HCl, 10 mM Boric acid, 0.1 mM EDTA, pH 8.0) were carried out at 10 mA and 5-8 V/cm. The denaturing gel was obtained from a solution containing 19% acrylamide, 1% bis(acrylamide), 7M Urea, 10 mM Tris.HCl, 10 mM Boric acid, 0.1 mM EDTA and 0.07% ammonium persulfate, pH 7.5 and carried out at 15 mA and 25-30 V/cm in TBE buffer. For both native and denaturing gels 0.1% bromophenol blue and 0.1% xylene cyanol blue solutions in water were used as references mixed with 50% glycerol and formamide respectively.

Physico-chemical measurements. For all measurements, the oligonucleotide solutions were heated to 70° C for 3 min and then allowed to cool down to 20°C for 30 min. They were equilibrated overnight at 4° C.

Melting measurements. UV melting profiles were obtained by scanning A_{260} absorbance versus temperature with a heating rate of 1.0° C / min in the temperature range 15 - 70° C (entries # 1 & 2, Table 1).. The T_m values were calculated from the first derivative of the melting curves with an accuracy of ±0.2° C. The duplex and hairpin melting experiments were carried out in buffer A: 20 mM Na_2HPO_4 / NaH_2PO_4, 1.0 M NaCl at pH 7.3. The extinction coefficients for oligonucleotides **1-5, 8-14** were calculated with the nearest-neighbour approximation.[34] In the case of the tethered oligomers **8** & **9**, the contribution of the aromatic moieties towards their extinction coefficients at 260 nm were estimated from the UV spectra of 1μmol solutions of polyarenes **6** & **7**.

Circular Dichroism Spectra. All CD experiments were recorded from 320 to 220 nm in 0.2 cm path length cuvettes using 10.4 mM strand concentration in 600 ml of buffer A. For CD spectra of the duplexes and hairpin the temperature was maintained at 10° C by circulating thermostated water through the cuvette holder. The samples were equilibrated at the required temperature for 10 min before recording the spectra. Each spectrum was an average of two scans with the buffer blank subtracted, which was also an average of two scans at the same scan speed (10 nm/min). The time constant and the sensitivity used were 16 sec and 20 x 10^{-2} m°/cm respectively. Each point in the spectra was manually fed into the Profit software in a Macintosh, where the spectra was smoothened using a 3-point average. The CD spectra was converted to $\Delta\varepsilon$ and reported as per mole of residues.

Acknowledgements

We thank Swedish Natural Science Research Council (NFR), Swedish Board for Technical Development (NUTEK) and Swedish Engineering Research Council (TFR) for generous financial

support. We also thank the Wallenbergstiftelsen, Forskningsrådsnämnden, and University of Uppsala for funds for the purchase of 600 and 500 MHz Bruker DRX NMR spectrometers.

References

(1) Lima, W. F.; Monia, B. P.; Ecker, D. J.; Freier, S. M. *Biochemistry* **1992**, *31*, 12055-12061.
(2) Milner, N.; Mir, K. U.; Southern, E. M. *Nature Biotechnology* **1997**, *15*, 537-541.
(3) Birikh, K. R.; Berlin, Y. A.; Soreq, H.; Eckstein, F. *RNA* **1997**, *3*, 429-437.
(4) Lima, W. F.; Brown-Driver, V.; Fox, M.; Hanecak, R.; Bruice, T. W. *J. Biol. Chem.* **1996**, *272*, 626-638.
(5) Ho, S. P.; Bao, Y.; Lesher, T.; Malhotra, R.; Ma, L. Y.; Fluharty, S. J.; Sakai, R. R. *Nature Biotechnology* **1998**, *16*, 59-62.
(6) Misra, R. K.; Tinevez, R. L.; Toulme, J. J. *Proc. Natl. Acad. Sci. USA* **1996**, *93*, 10679-10684.
(7) Toulme, J. J.; Le Tinevez, R.; Boiziau, C.; Dausse, E. *Nucleic Acids Symp. Ser.* **1997**, *36*, 39-41.
(8) Lieber, A.; Strauss, M. *Mol. Cell. Biol.* **1995**, *15*, 540-551.
(9) Puri, N.; Zamaratski, E.; Sund, C.; Chattopadhyaya, J. *Tetrahedron* **1997**, *53*, 10409-10432.
(10) Puri, N.; Chattopadhyaya, J. *J. Org. Chem* **1998**, submitted.
(11) McDowell, J. A.; Turner, D. H. *Biochemistry* **1996**, *35*, 14077-14089.
(12) Biswas, R.; Wahl, M. C.; Ban, C.; Sundaralingam, M. *J. Mol. Biol.* **1997**, *267*, 1149-1156.
(13) Biswas, R.; Sundaralingam, M. *J. Mol. Biol.* **1997**, *270*, 511-519.
(14) Gervais, V.; Cognet, J. A. H.; Le Bret, M.; Sowers, L. C.; Fazakerley, G. V. *Eur. J. Biochem.* **1995**, *228*, 279-290.
(15) Arnold, F. H.; Wolk, S.; Cruz, P.; Tinoco, I., Jr. *Biochemistry* **1987**, *26*, 4068-4075.
(16) Maskos, K.; Gunn, B. M.; LeBlanc, D. A.; Morden, K. M. *Biochemistry* **1993**, *32*, 3583-3595.
(17) Zuker, M. *Methods Mol. Biol.* **1994**, *25*, 267-294.
(18) Mathews, D. H.; Andre, T. C.; Kim, J.; Turner, D. H.; Zuker, M. *Am. Chem. Soc. Symp. Ser.* **1998**, *682*, 246-257.
(19) Marky, L. A.; Breslauer, K. J. *Biopolymers* **1987**, *26*, 1601-1620.
(20) Sakata, T.; Hiroaki, H.; Oda, Y.; Tanaka, T.; Ikehara, M.; Uesugi, S. *Nucl. Acids Res.* **1990**, *18*, 3831-3839.
(21) Serra, M. J.; Turner, D. H. *Meth. Enzymol.*; 1995; Vol. 259, pp 242-261.
(22) Xodo, L. E.; Manzini, G.; Quadrifoglio, F.; van der Marel, G. A.; van Boom, J. H. *Biochemistry* **1988**, *27*, 6321-6326.
(23) Zuo, E. T.; Tanious, F. A.; Wilson, W. D.; Zon, G.; Tan, G.; Wartell, R. M. *Biochemistry* **1990**, *29*, 4446-4456.
(24) Toulme, J. J.; Tinevez, R. L.; Brossalina, E. *Biochimie* **1996**, *78*, 663-673.
(25) Matveeva, O.; Felden, B.; Audlin, S.; Gesteland, R. F.; Atkins, J. F. *Nucl. Acids Res.* **1997**, *25*, 5010-5016.
(26) Wang, S.; Kool, E. T. *Biochemistry* **1995**, *34*, 4125-4132.
(27) Hunter, W. N.; Brown, T.; Kneale, G.; Anand, N. N.; Rabinovich, D.; Kennard, O. *J. Biol. Chem.* **1987**, *262*, 9962-9970.
(28) SantaLucia, J., Jr. *Proc. Natl. Acad. Sci. USA* **1998**, *95*, 1460-1465.
(29) Allen, F. S.; Gray, D. M.; Roberts, G. P.; Tinoco, I., Jr *Biopolymers* **1972**, *11*, 853-879.
(30) Summers, M. F.; Byrd, R. A.; Gallo, K. A.; Samsom, C. J.; Zon, G.; Egan, W. *Nucl. Acids Res.* **1985**, *13*, 6375-6386.
(31) Allawi, H. T.; SantaLucia, J., Jr *Biochemistry* **1997**, *36*, 10581-10594.
(32) Muller, U. R.; Fitch, W. M. *J. Theor. Biol.* **1985**, *117*, 119-126.
(33) Lyttle, M. H.; Wright, P. B.; Sinha, N. D.; Bain, J. D.; Chamberlin, A. R. *J. Org. Chem.* **1991**, *56*, 4608-4615.
(34) Fasman, G. *In Handbook of Biochemistry and Molecular Biology, Vol. I*; CRC Press: Ohio. **1975**, pp 589.